CHEMIJA
2023. Vol. 34. No. 1. P. 1–7

ISSN 0235-7216 eISSN 2424-4538
DOI: https://doi.org/10.6001/chemija.2023.34.1.1

Formation of tethered bilayer lipid membranes on gold surface probed by *in situ* SEIRAS

Vaidas Pudžaitis[1],

Martynas Talaikis[2],

Gintaras Valinčius[2],

Gediminas Niaura[1, 2*]

[1] *Department of Organic Chemistry, Center for Physical Sciences and Technology, 3 Saulėtekio Avenue, 10257 Vilnius, Lithuania*

[2] *Department of Bioelectrochemistry and Biospectroscopy, Institute of Biochemistry, Life Sciences Center, Vilnius University, 7 Saulėtekio Avenue, 10257 Vilnius, Lithuania*

Tethered bilayer lipid membranes (tBLMs) are versatile platforms for the analysis of biochemical and biophysical processes at biological membranes. To control the stability and functional properties of these artificial constructions, molecular-level knowledge on the organization and structure is required. We used surface-enhanced infrared absorption spectroscopy (SEIRAS) to elucidate the *in situ* formation of tBLMs on a gold substrate. The alkyl chains of long-chain anchoring thiol in a mixed self-assembled monolayer after 60 min of incubation in an adsorption methanol-d_4 solution was found to be in a disordered state. Spectroscopic data revealed the complete formation of a bilayer after 60 min of incubation of a mixed anchoring monolayer in a phosphate buffer solution containing vesicles formed from partially deuterated lipid DPPC-d_{62} and cholesterol-d_7. The temporal evolution of absorption bands from the lipid, anchoring mixed monolayer thiol, and water with increasing the bilayer formation time in the phosphate buffer solution containing vesicles revealed a two-stage process. Firstly, the adsorption of lipid molecules with a simultaneous withdrawal of water takes place at the interface. Secondly, the transformation of alkyl chains of the anchoring monolayer due to the insertion and interaction of lipids with the monolayer proceeds.

Keywords: tethered bilayer lipid membrane, SAM, surface-enhanced infrared absorption spectroscopy, gold

INTRODUCTION

Tethered bilayer lipid membranes (tBLMs) assembled on a gold substrate serve as a versatile platform to mimic biochemical and biophysical processes at biological membranes [1–3]. Such structures are also promising for the construction of biosensors and biomedical screening applications [4–6]. The important advantage of these membranes, compared with other constructs, is the presence of an exchangeable solution reservoir between the solid substrate (gold electrode) and the bilayer [7–9]. The presence of such reservoir ensures the incorporation and stability of transmembrane proteins [10, 11]. In addition, the separation of bilayer from the solid substrate by a flexible and hydrophilic layer with water assures the mobility of inserted proteins required for their function. Usually, a tBLM structure is designed in two steps. First, the bilayer anchoring layer on the solid substrate is formed from polar peptides, carbohydrates, polymers, or self-assembled monolayers (SAMs) of thiol molecules [5, 9, 12–14]. Secondly, the lipid vesicles fuse on the layer of tethered compounds and arrange a planar lipid bilayer. The SAM approach offers advantages due to the ease of preparation, reproducibility, a low defect density, and the control of bilayer fluidity. In this case, the convenient

* Corresponding author. Email: gediminas.niaura@ftmc.lt

solid substrate is gold because of its strong affinity to a sulfur atom and the formation of a robust Au–S bond. To establish a water reservoir between the electrode and bilayer, the mixed SAM constituted by a short thiol with a terminal hydroxyl functional group and long-chain lipid anchoring thiol is formed on the gold substrate [8, 9].

The stability and functional properties of tBLM rely toughly on the composition and structure of anchoring SAM [11, 15–19]. However, the molecular level knowledge on the structure and formation of a mixed monolayer in a solution still remains scarce largely because of a limited number of available techniques providing molecular information from the electrode/solution interface. Surface-enhanced infrared absorption spectroscopy (SEIRAS) is one of the most promising tools for probing the structure, adsorption peculiarities, and the orientation of adsorbed molecules at the electrochemical interface with molecular specificity and submonolayer sensitivity [20, 21]. The analysis of a secondary structure of adsorbed peptides, the conformation of self-assembled monolayers, and the function of surface attached biosensors were successfully accomplished by employing of the *in situ* SEIRAS approach [20, 21–23].

The present work has been aimed at *in situ* SEIRAS probing the development of an anchoring monolayer and the formation of a bilayer at a gold electrode.

EXPERIMENTAL

Materials

Chemical reagents and solvents such as acetone (99.9%), CH_3COONa (98.5%), H_2O_2 (30%), Na_2SO_3 (98%), NH_4Cl (99.5%), NH_4F (98%), HF (48%), $Na_2S_2O_3{\cdot}5H_2O$ (ACS grade) and $NaAuCl_4{\cdot}2H_2O$ (99%) were purchased from Sigma-Aldrich (St. Louis, MO, USA), Fluka (Buchs, Switzerland) and Merck (Darmstadt, Germany). Aqueous solutions were prepared using deionized water (18.2 MΩ·cm) from the Direct-Q 3UV purification system (Merck, Germany). The silicon crystal for SEIRAS was bought from Pike Technologies (USA).

SEIRAS measurement

SEIRAS substrate preparation and experiment details have been described elsewhere [22]. In short, the polished face-angled Si crystal was reduced with 1 mL HF (2 wt%) and then coated with an Au film by applying a plating mixture for 4 min at room temperature. Then the film was etched with a concentrated aqua regia solution, which was followed by the second Au plating step. Such an approach results in an increased mechanical resistance of the gold layer [24]. The Au plating solution comprised equal volumes of the solutions: 1) 0.15 M Na_2SO_3, 0.05 M $Na_2S_2O_3$ and 0.05 M NH_4Cl, 2) NH_4F (20 wt%), 3) HF (2 wt%) and 4) $NaAuCl_4$ (0.03 M). The gold layer was additionally cleaned and activated by electropolishing in a N_2-purged pH 5.8 sodium acetate solution (0.1 M). Cyclic voltammetry (CV) scans were performed using a PGSTAT101 potentiostat (Methrom, USA) starting from ±200 mV of the open circuit potential (OCP) at 20 mV/s speed. The upper potential limit was increased by 100 mV every three full cycles until the gold oxidation at around 1.0 V. SEIRAS measurements were carried out using a spectrometer Vertex 80v (Bruker, Germany) equipped with a liquid nitrogen-cooled narrow-band LN-MCT (HgCdTe) detector. The spectral resolution was set to 4 cm^{-1}, the aperture to 2 mm, 50 sample scans and 100 background scans were co-added. The freshly prepared SEIRAS substrate was assembled into a VeeMax III accessory with a Jackfish cell J1F (Pike Technologies, USA). The incident angle for an ATR unit was set to 63 degrees. The spectrometer was purged with dry air overnight.

SAM and tBLM formation

Approximately 0.2 mL of either WC14 (20-(tetradecyloxy)-3,6,9,12,15,18,22-heptaoxahexatriacontane-1-thiol; synthesized in-house), ME (2-mercaptoethanol), or WC14/ME (30/70 mol%) thiol solution in ethanol or methanol-d_4 (0.2 mM) were injected into the cell and SEIRAS spectra were measured immediately every 15–120 s. After a couple of hours, the cell was thoroughly rinsed with ethanol or methanol-d_4 and then with a phosphate buffer solution (PBS, 0.05 M with 0.1 M Na_2SO_4, pH 4.5). The tBLM was formed by injecting approximately 0.2 mL of a multilamellar vesicle solution (1 mM) of 1,2-dipalmitoyl-d62-sn-glycero-3-phosphocholine and cholesterol-d_7 mixture DPPC-d_{62}/cholesterol-d_7 (Avanti Polar Lipids, Inc., USA) according to the procedure detailed in Ref. [25] and immediately followed by SEIRAS.

RESULTS AND DISCUSSION

Formation of mixed anchoring SAM on gold

Figure 1 shows the molecular structure of long chain (WC14) and short chain (ME) thiols used for the construction of bilayer anchoring mixed SAM. In such a way assembled tBLM was previously used for the analysis of the structure and function of pore-forming toxins [26, 27] and the interaction of proteins with a membrane [8]. The optimal composition of the adsorption solution for the self-assembly of the anchoring monolayer was found to be WC14/ME (30/70 mol%) [19].

Figure 2 shows the development of SEIRAS spectra during the self-assembly of mixed bilayer-anchoring monolayer from the methanol-d_4 (CD_3–OD) solution due to the introduction of thiol molecules WC14/ME (30/70 mol%). After 60 min of incubation, strong bands at 1464, 1350 and 1157 cm^{-1} appeared in the fingerprint spectral

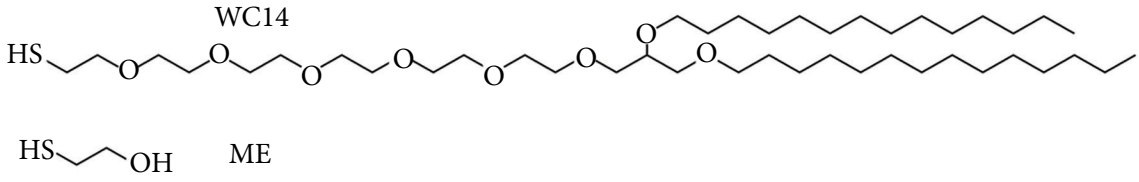

Fig. 1. Chemical structures of mixed SAM forming thiols, WC14 (20-(tetradecyloxy)-3,6,9,12,15,18,22-heptaoxahexatriacontane-1-thiol) and ME (2-mercaptoethanol)

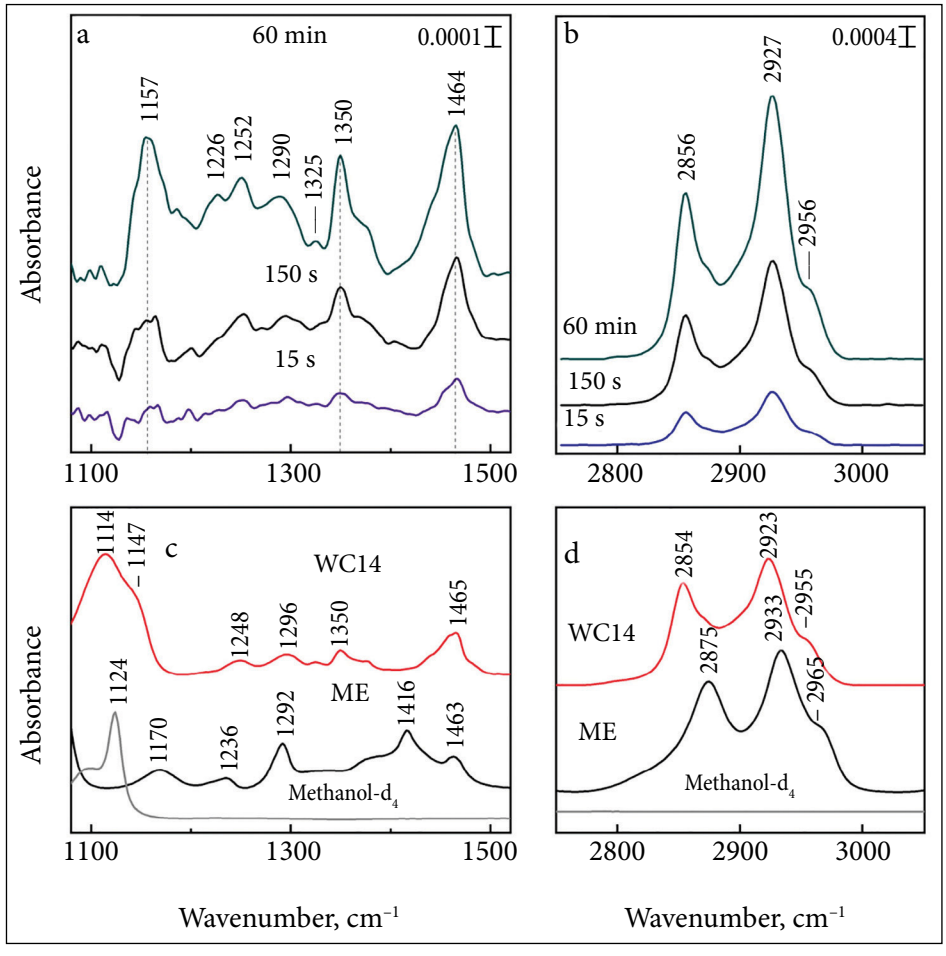

Fig. 2. SEIRAS spectra captured at different times during the formation of mixed SAM (WC14/ME, 30/70 mol%) from methanol-d_4 (CD_3–OD) solution in the fingerprint spectral region (a) (1080–1520 cm^{-1}) and (b) the C–H stretching frequency region (2750–3050 cm^{-1}). The reference spectrum was obtained in pure methanol-d_4 before the introduction of thiol molecules in the working solution. (c, d) The infrared spectra of solid state WC14, bulk ME and solvent methanol-d_4 in the corresponding spectral regions

region (Fig. 2a). The band near 1464 cm^{-1} belongs to the predominant CH_2 scissoring deformation vibration of alkyl chains. The band is broad because of some contribution from ethylene glycol (EG, $–CH_2–CH_2–O–$) units in the gauche conformation and EG groups in an amorphous structure expected at 1463–1465 and 1460 cm^{-1}, respectively [28]. The intense feature near 1350 cm^{-1} was assigned to the wagging vibration of the CH_2 groups of EG units in the gauche conformation [28]. The broad and intense absorption band at 1157 cm^{-1} belongs to the characteristic asymmetric stretching vibrational mode of C–O–C group, ν_{as}(C–O–C) [18, 19, 28–35]. It should be noted that the shape of this peak can be affected by a strong IR absorption of the Si prism at wavenumbers below 1000 cm^{-1} [36]. The peak position of this mode provides information on the structure of the poly(ethylene glycol) (PEG) part of the molecule [18, 29–35]. A relatively high frequency value observed in this work indicates the presence of a predominantly amorphous structure [28, 35]. However, the width of this band in the surface spectrum is considerably smaller compared with the corresponding band of WC14 in the solid state infrared spectrum near 1114/1147 cm^{-1} (Fig. 2c). This indicates the prevalence of one relatively uniform conformational form of PEG chains in the monolayer. It was previously demonstrated that such amorphous structure of the PEG chain in oligo(ethylene glycol)-terminated SAMs is highly solvated by water and able to prevent adsorption of proteins in contrast to the 'all-trans' conformation [28]. The formation of mixed SAM presented in Fig. 2 was performed in a methanol-d_4 ($CD_3–OD$) solution. Only one intense band near 1124 cm^{-1} belongs to the solvent molecules in the investigated spectral region (Fig. 2c). Thus, some spectral perturbations are expected in the vicinity of C–O–C stretching band due to the adsorption/desorption of solvent molecules during the self-assembly. In the high frequency region (Fig. 2b), the absorption bands due to the CH_2 symmetric [$\nu_s(CH_2)$] and asymmetric [$\nu_{as}(CH_2)$] stretching vibrations of methylene chains are visible near 2856 and 2927 cm^{-1}, respectively [18, 19]. The position of an asymmetric stretching band provides information on the ordering of alkyl chains. Thus, highly ordered SAMs exhibit the $\nu_{as}(CH_2)$ band in the frequency region 2917–2919 cm^{-1} [37–39], while disordering results in the frequency upshift. The peak positions of both bands in the surface spectra are higher by several wavenumbers compared with the solid state spectrum of WC14 (Fig. 2d) indicating a relatively disordered structure of the alkyl chains in the mixed monolayer. All bands observed in the SEIRAS spectra were assigned to the adsorbed WC14 compound; no spectral features for adsorbed ME were obtained. The prominent ME bands near 1416 and 2875 cm^{-1} (Fig. 2c, d) are not visible in the surface spectra (Fig. 2 a, b). The time-dependent spectral changes indicate an increase in the relative intensity of the ν_{as}(C–O–C) band near 1157 cm^{-1} of the PEG segment compared with the scissoring deformation band of CH_2 groups near 1464 cm^{-1} (Fig. 2a). This indicates the reorientation of molecules during the self-assembly process. Previous reflection-absorption infrared spectroscopy (RAIRS) studies revealed that the relative intensification of ν_{as}(C–O–C) mode reflects the more vertical alignment of WC14 molecule [18, 19].

Formation of a bilayer on a mixed anchoring monolayer on gold

Figure 3 shows the changes in the SEIRAS spectra during the formation of bilayer on mixed SAM in the spectral region from 2000 to 3700 cm^{-1}. The positive-going bands indicate the adsorption process, while the negative-going bands denote the withdrawal of the corresponding compounds from the interface. For the construction of bilayer, the multilamellar vesicle solution of deuterated

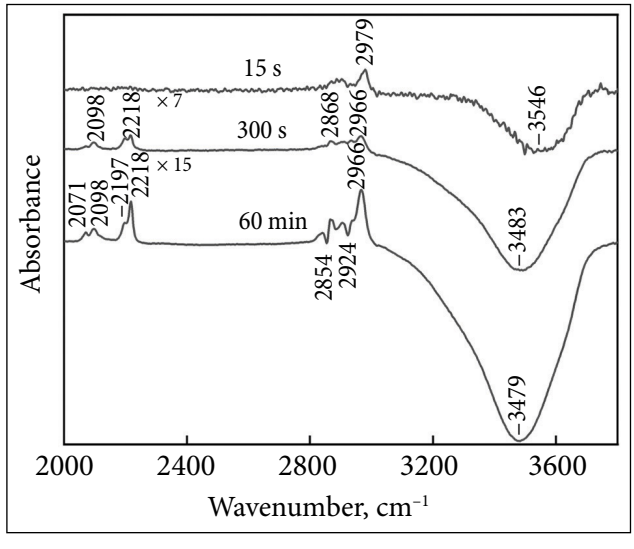

Fig. 3. SEIRAS-difference spectra captured at different times during the formation of the second layer (DPPC-d_{62}/cholesterol-d_7, 60/40 mol%) on mixed SAM (WC14/ME, 30/70 mol%) in an aqueous solution

phospholipid and cholesterol (DPPC-d_{62}/cholesterol-d_7) in the phosphate buffer solution was employed. The low intensity positive-going band near 2979 cm^{-1} due to the asymmetric stretching vibration of CH_3 group is visible after 15 s of bilayer formation. This band might be related to the orientation changes of the terminal methyl group of adsorbed WC14. Simultaneously, a broad negative-going band near 3546 cm^{-1} due to the O–H stretching vibration appears in the SEIRAS spectrum.

After 300 s of incubation, four positive-going bands due to the stretching vibrations of the CD_2 and CD_3 groups of DPPC-d_{62} appear at 2071, 2098, 2197 and 2218 cm^{-1}. The bands at 2071 and 2218 cm^{-1} were previously assigned to symmetric and asymmetric CD_3 stretching vibrations, respectively [$\nu_s(CD_3)$ and $\nu_{as}(CD_3)$], while the bands at 2098 and 2197 cm^{-1} were attributed to the symmetric and asymmetric stretching modes of CD_2 group, respectively [$\nu_s(CD_2)$ and $\nu_{as}(CD_2)$] [40–43]. Figure 4 displays the infrared absorption spectra of bulk chol-d_7 and DPPC-d_{62}. Compared with the bulk infrared spectrum, the intensities of CD_3 vibrational modes are enhanced in the surface spectrum. In addition, some contribution from cholesterol-d_7 may take place for the observed 2218 cm^{-1} band in the SEIRAS spectrum (Fig. 3). The increase of incubation time (60 min) results in the relative intensification of 2071, 2218 cm^{-1} and 2966 cm^{-1} bands and the negative-going water absorption feature near 3479 cm^{-1}. Importantly, the peak position of negative-going water band shifts to lower wavenumbers with increasing incubation time, indicating that during the first few minutes, water molecules characterized by fewer hydrogen bonds leave the interface. This is followed by water molecules with a higher quantity of hydrogen bonds at a later stage of tBLM formation. The relative intensification of CD_3 stretching bands might be related with the penetration of CD_3 group close to the surface and changes in the alignment of the alkyl chains of DPPC-d_{62}. In addition, the negative-going features are visible at 2854 [$\nu_s(CH_2)$] and 2924 cm^{-1} [$\nu_{as}(CH_2)$] after 60 min of bilayer formation. These bands are associated with the changes in the alignment of the alkyl chains of adsorbed WC14 molecules. Lowering relative intensity and the shift to the lower wavenumbers of stretching CH_2 bands indicate the more perpendicular with respect to the surface orientation of WC14 alkyl chains and the increase in ordering, respectively [37–39].

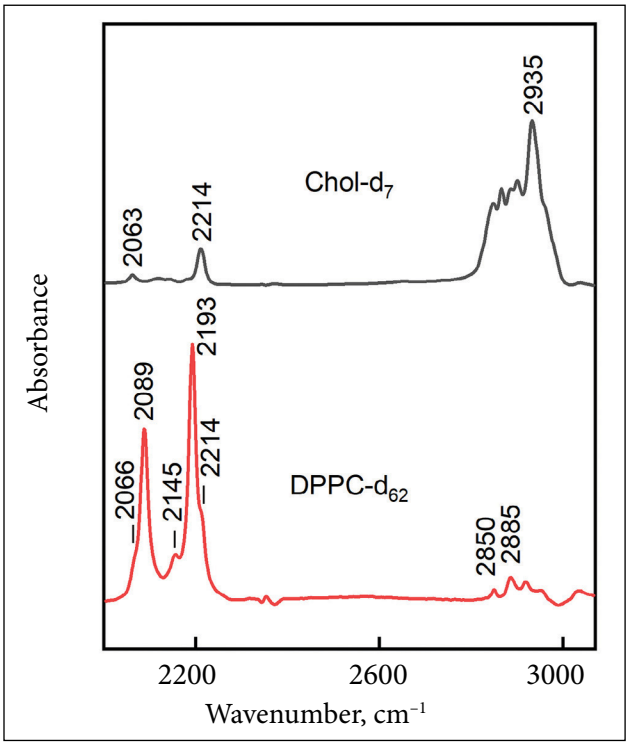

Fig. 4. Infrared absorption spectra of the bulk compounds employed for the formation of bilayer: cholesterol-d_7 (Chol-d_7) and DPPC-d_{62}

The temporal evolution of the parameters of SEIRAS bands with increasing the bilayer formation time is displayed in Fig. 5. One can see that during the first 20 min, the temporal behaviour of spectral bands related with the DPPC-d_{62} $\nu_{as}(CD_3)$ mode and the anchoring monolayer $\nu_{as}(CH_2)$ band is different. The water withdrawing from the surface behaviour is similar with the DPPC-d_{62} changes. For more quantitative analysis, the experimental data were fitted with the Boltzmann model

$$y(x) = \frac{A_1 - A_2}{1 + e^{(x - x_0)/dx}} + A_2, \quad (1)$$

where A_1 and A_2 are initial and final values, and x_0 is the time of process midpoint. The x_0 was found to be 6.0 ± 0.35 min and 4.5 ± 0.11 min for $I\nu_{as}(CD_3)$ and $A\nu(OH)$ alterations, respectively, and 9.9 ± 0.31 min for $I\nu_{as}(CH_2)$ changes. Thus, the SEIRAS data indicate that the formation of bilayer proceeds through the two-step mechanism. The adsorption of DPPC-d_{62}/cholesterol-d_7 lipid bilayer at the mixed anchoring monolayer takes place at the first stage with a simultaneous withdrawal of water from the interface, while the transformation of the alkyl chains of WC14 in the monolayer due to the insertion and interaction of bilayer proceeds at the second stage.

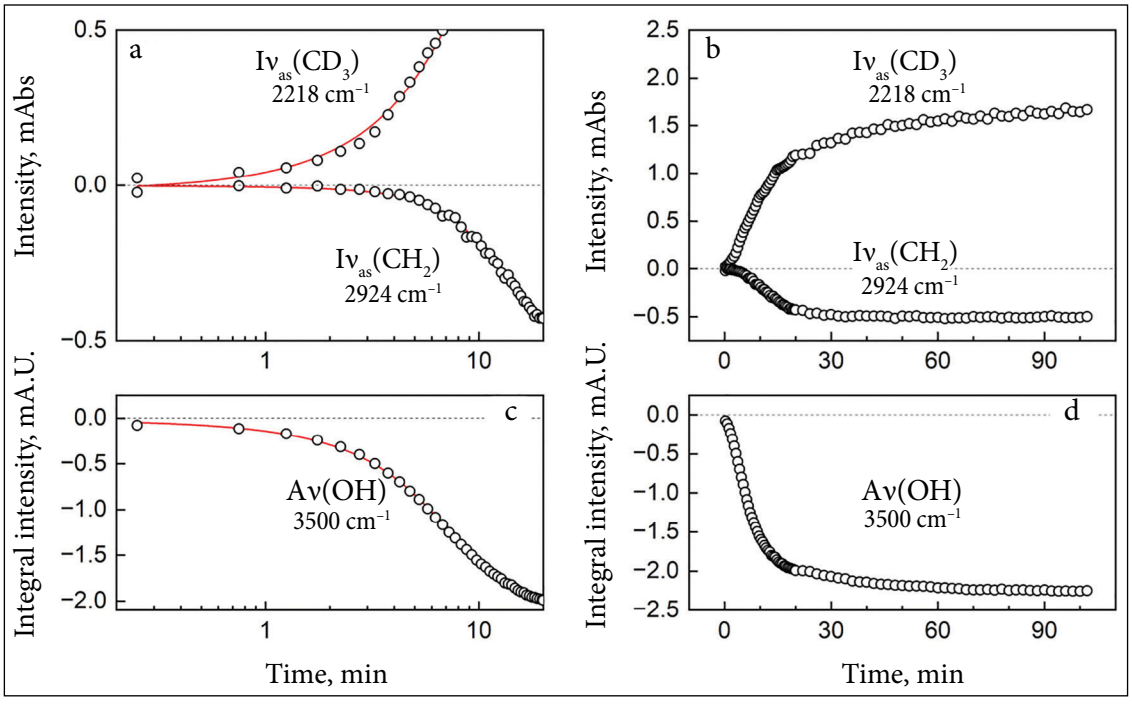

Fig. 5. (a) Temporal evolution of the spectral mode intensities related to the DPPC-d_{62} adsorption and reorientation on a surface [Iν$_{as}$(CD$_3$)] and the reorientation of anchoring molecules [Iν$_{as}$(CH$_2$)] during the tBLM formation for the first 20 min and (b) during the period of 105 min. (c) Temporal evolution of the ν(OH) integral intensity related to the removal of water molecules from the surface during the tBLM formation for the first 20 min and (d) during the period of 105 min. Red lines represent the fitting of the experimental data with the Boltzmann model, which yields the 50% process threshold at 6.0 ± 0.35 min [Iν$_{as}$(CD$_3$)], 9.9 ± 0.31 min [Iν$_{as}$(CH$_2$)] and 4.5 ± 0.11 min [Aν(OH)]

Figures 5b and d show that after approximately 60 min the spectral changes due to the formation of bilayer are essentially complete.

CONCLUSIONS

In this study, we used surface-enhanced infrared absorption spectroscopy (SEIRAS) to monitor two processes related to the construction of tethered bilayer lipid membranes (tBLMs) on the gold substrate: the formation of the anchoring mixed self-assembled monolayer and the development of the lipid bilayer at mixed SAM. We found that the ethyleneglycol chains of long-chain thiol in SAM are in the predominant amorphous state, while the alkyl chains are in the disordered state providing the required flexibility for the formation of bilayer. The bilayer lipid formation process takes place through the two stages: the adsorption of lipids with the simultaneous desorption of water from the interface and insertion/interaction of lipids with the monolayer resulting in the structural changes of the alkyl chains of SAM. We found that the development of lipid bilayer ends after about 60 min after the introduction of the vesicles composed of the mixture of partially deuterated compounds DPPC-d_{62}/cholesterol-d_7.

ACKNOWLEDGEMENTS

This article is dedicated to the anniversary of Prof. Albertas Malinauskas.

Received 13 January 2023
Accepted 30 January 2023

References

1. S. Rebaud, O. Maniti, A. P. Girard-Egrot, *Biochimie*, **107**, 135 (2014).
2. J. Lipkowski, *Phys. Chem. Chem. Phys.*, **12**, 13874 (2010).
3. A. P. Girard-Egrot, O. Maniti, *Appl. Sci.*, **11**, 4876 (2021).
4. T. Penkauskas, G. Preta, *Biochimie*, **157**, 131 (2019).
5. J. A. Jackman, W. Knoll, N.-J. Cho, *Materials,* **5**, 2637 (2012).
6. B. A. Cornell, V. L. B. Braach-Maksvytis, L. G. King, et al., *Nature*, **387**, 580 (1997).
7. G. Krishna, J. Schulte, B. A. Cornell, R. Pace, L. Wieczorek, P. D. Osman, *Langmuir*, **17**, 4858 (2001).

8. G. Valincius, D. J. McGillivray, W. Febo-Ayala, D. J. Vanderah, J. J. Kasianowicz, M. Losche, *J. Phys. Chem. B*, **110**, 10213 (2006).
9. D. J. McGillivray, G. Valincius, D. J. Vanderah, et al., *Biointerfaces*, **2**, 21 (2007).
10. B. W. Koenig, S. Kruger, W. J. Orts, et al., *Langmuir*, **12**, 1343 (1996).
11. H. Basit, A. Van der Heyden, C. Gondran, B. Nysten, P. Dumy, P. Labbe, *Langmuir*, **27**, 14317 (2011).
12. R. Naumann, T. Baumgart, P. Graber, A. Jonczyk, A. Offenhausser, W. Knoll, *Biosens. Bioelectron*., **17**, 25 (2002).
13. M. Tanaka, E. Sackmann, *Nature*, **437**, 656 (2005).
14. W. Knoll, I. Koeper, R. Naumann, E.-K. Sinner, *Electrochim. Acta*, **53**, 6680 (2008).
15. J. Andersson, M. A. Fuller, K. Wood, S. A. Holt, I. Koper, *Phys. Chem. Chem. Phys*., **20**, 12958 (2018).
16. M. Talaikis, G. Valincius, G. Niaura, *J. Phys. Chem. C*, **124**, 19033 (2020).
17. M. Talaikis, O. Eicher-Lorka, G. Valincius, G. Niaura, *J. Phys. Chem. C*, **120**, 22489 (2016).
18. R. Budvytyte, G. Valincius, G. Niaura, et al., *Langmuir*, **29**, 8645 (2013).
19. B. Rakowska, T. Ragaliauskas, M. Mickevicius, et al., *Langmuir*, **31**, 846 (2015).
20. X. Yang, Z. Sun, T. Low, et al., *Adv. Mater*., **30**, 1704896 (2018).
21. J. Li, B. Zheng, Q.-W. Zhang, et al., *J. Anal. Test*., **1**, 8 (2017).
22. V. Pudžaitis, M. Talaikis, R. Sadzevičienė, L. Labanauskas, G. Niaura, *Materials*, **15**, 7221 (2022).
23. E. Forbrig, J. K. Staffa, J. Salewski, M. A. Mroginski, P. Hildebrandt, J. Kozuch, *Langmuir*, **34**, 2373 (2018).
24. M. Yaguchi, T. Uchida, K. Motobayashi, M. Osawa, *J. Phys. Chem. Lett*., **7**, 3097 (2016).
25. T. Ragaliauskas, M. Mickevicius, B. Rakovska, et al., *Biochim. Biophys. Acta Biomembr*., **1859**, 669 (2017).
26. D. J. McGillivray, G. Valincius, F. Heinrich, et al., *Biophys. J*., **96**, 1547 (2009).
27. R. Budvytyte, M. Pleckaityte, A. Zvirbliene, D. J. Vanderah, G. Valincius, *PloS One*, **8**, e82536 (2013).
28. P. Harder, M. Grunze, R. Dahint, G. M. Whitesides, P. E. Laibinis, *J. Phys. Chem. B*, **102**, 426 (1998).
29. M. Kobayashi, M. Sakashita, *J. Chem. Phys*., **96**, 748 (1992).
30. D. J. Vanderah, C. P. Pham, S. K. Springer, V. Silin, C. W. Meuse, *Langmuir*, **16**, 6527 (2000).
31. D. J. Vanderah, C. W. Meuse, V. Silin, A. L. Plant, *Langmuir*, **14**, 6916 (1998).
32. D. J. Vanderah, G. Valincius, C. W. Meuse, *Langmuir*, **18**, 4674 (2002).
33. D. J. Vanderah, J. Arsenault, H. La, et al., *Langmuir*, **19**, 3752 (2003).
34. D. J. Vanderah, R. S. Gates, V. Silin, et al., *Langmuir*, **19**, 2612 (2003).
35. D. J. Vanderah, T. Parr, V. Silin, et al., *Langmuir*, **20**, 1311 (2004).
36. X.-K. Xue, J.-Y. Wang, Q.-X. Li, Y.-G. Yan, J-H. Liu, W.-B. Cai, *Anal. Chem*., **80**, 166 (2008).
37. M. D. Porter, T. B. Bright, D. L. Allara, C. E. D. Chidsey, *J. Am. Chem. Soc*., **109**, 3559 (1987).
38. P. E. Laibinis, G. M. Whitesides, D. L. Allara, Y.-T. Tao, A. N. Parikh, R. G. Nuzzo, *J. Am. Chem. Soc*., **113**, 7152 (1991).
39. A. N. Parikh, D. Allara, *J. Chem. Phys*., **96**, 927 (1992).
40. S. Sunder, D. Cameron, H. H. Mantsch, H. J. Bernstein, *Can. J. Chem*., **56**, 2121 (1978).
41. G. Ma, H. C. Allen, *Langmuir*, **22**, 5341 (2006).
42. R.-J. Feng, X. Li, Z. Zhang, Z. Lu, Y. Guo, *J. Chem. Phys*., **145**, 244707 (2016).
43. C. W. Meuse, G. Niaura, M. L. Lewis, A. L. Plant, *Langmuir*, **14**, 1604 (1998).

Vaidas Pudžaitis, Martynas Talaikis, Gintaras Valinčius, Gediminas Niaura

PAKABINAMŲ BISLUOKSNIŲ MEMBRANŲ FORMAVIMOSI ANT AUKSO PAVIRŠIAUS TYRIMAS *IN-SITU SEIRAS* METODU

S a n t r a u k a

Pakabinamos bisluoksnės lipidinės membranos (tBLM), imobilizuotos aukso paviršiuje, plačiai pritaikomos tiriant biocheminius ir biofizikinius procesus, vykstančius prie ląstelės membranos bei konstruojant biojutiklius. Norint geriau valdyti tBLM savybes, funkcionalumą, stabilumą ir suderinamumą su membraniniais baltymais, būtina suprasti molekulinius procesus, vykstančius šiose membranose ir membranų inkariniuose sluoksniuose. Šiame darbe buvo tirtas tBLM formavimasis ant aukso paviršiaus *in-situ* paviršiaus sustiprintos infraraudonosios sugerties spektroskopijos (SEIRAS) metodu. Pirmiausia buvo suformuotas mišrus savitvarkis monosluoksnis (SAM), sudarytas iš ilgagrandžio inkarinio WC14 junginio ir paviršiaus skiediklio 2-merkaptoetanolio. SEIRAS duomenimis, etilenglikolio ir alkilinių grandinių struktūra inkariniame WC14 junginyje išlieka netvarki monosluoksnį formuojant metanolio-d_4 tirpale 60 min. Nustatyta, kad lipidų bisluoksnis susiformuoja per 60 min liejant daugiasluoksnes DPPC-d_{62} ir cholesterolio-d_7 liposomas ant mišraus SAM fosfatiniame buferiniame tirpale. Bisluoksnio formavimosi eigą sudaro du etapai. Pirmiausia prie paviršiaus priartėja ir adsorbuojasi lipidų molekulės, išstumdamos iš fazių ribos vandenį. Paskui inkarinės savitvarkio monosluoksnio molekulės persitvarko taip, kad jų alkilinės grandinės įsiterptų į lipidinį bisluoksnį, imobilizuodamos jį paviršiuje.